J. Pharm. Pharmacol. 1997, 49: 698–705
Received December 2, 1996
Accepted February 17, 1997

The Ligand-binding Site of Buspirone Analogues at the 5-HT_{1A} Receptor

INGEBRIGT SYLTE, ZDZISLAW CHILMONCZYK*, SVEIN G. DAHL, JACEK CYBULSKI* AND ØYVIND EDVARDSEN

*Department of Pharmacology, Institute of Medical Biology, University of Tromsø, N-9037 Tromsø, Norway, and *Pharmaceutical Research Institute, 8 Rydygiera Street, 01-793 Warszawa, Poland*

Abstract

A three-dimensional model of the 5-HT_{1A} receptor in man was constructed by molecular-modelling techniques and used to study the molecular interactions of a series of buspirone analogues with the 5-HT_{1A} receptor by molecular-mechanical-energy minimization and molecular-dynamics simulations.

The receptor has seven trans-membrane α helices (TMHs) organized according to the electron-density-projection map of visual rhodopsin, and includes all loops between TMHs and the N- and C-terminal parts. The best fit between the buspirone analogues and the receptor model was obtained with the quinolinyl part of the ligand molecules interacting with amino acids in TMH6, the imide group interacting with amino acids in TMH2, TMH3 and TMH7, and the carbonyl groups hydrogen-bonded with Ser86 and Ser393. The ligand-binding rank order deduced from the experimentally determined inhibition constant was reproduced by calculation of receptor-binding energies of the buspirone analogues.

The models suggest that steric hindrance and repulsive forces between the receptor and the imide group of the buspirone analogues are the most important determinants of ligand-binding affinity for discriminating between these ligands.

By acting on specific cell-surface receptors, the neurotransmitter 5-hydroxytryptamine (5-HT) is involved in various physiological and pathophysiological processes. The receptors activated by 5-HT have been divided into seven classes, and at least fifteen different 5-HT receptor-subtype genes have been characterized (Hoyer et al 1994). Six 5-HT receptor subtypes are members of the 5-HT_1 family; these are designated the 5-HT_{1A}, 5-HT_{1B}, 5-HT_{1DA}, 5-HT_{1DB}, 5-HT_{1E} and 5-HT_{1F} receptors. Among these the 5-HT_{1A} receptor is that which is best characterized, mainly because of the availability of a selective 5-HT_{1A} receptor agonist, 8-hydroxy-2-(dipropylamino)tetralin.

Except for the 5-HT_3 receptor, the 5-HT receptors are members of the family of guanine nucleotide-binding regulatory protein (G protein)-coupled receptors (Hoyer et al 1994). G protein-coupled neurotransmitter receptors are integral membrane proteins believed to consist of seven trans-membrane-spanning α helices (TMHs), connected by three intracellular and three extracelluar loops (Schwartz 1994). All available information indicates that the TMHs form a central core, by analogy with rhodopsin, and that binding of small molecules to catecholamine receptors involves amino acids within the central core of the TMHs (Schwartz 1994).

Clinical trials have shown that the partial 5-HT_{1A} receptor agonist, buspirone, which is structurally unrelated to the benzodiazepines, has an anxiolytic effect similar to that of diazepam (Goa & Ward 1986; Traber & Glaser 1987). Buspirone had an advantage over the benzodiazepines in that it did not cause sedation and was not addictive and thus had no associated withdrawal syndrome (Goa & Ward 1986; Peroutka 1995). It was later reported that buspirone and other 5-HT_{1A} receptor agonists also have anti-depressive properties (Wieland & Lucki 1990).

Correspondence: I. Sylte, Department of Pharmacology, Institute of Medical Biology, University of Tromsø, N-9037 Tromsø, Norway.

These observations suggested that buspirone, and possibly also other structurally related 5-HT_{1A} receptor ligands, might be useful agents for treatment of anxiety and depression, and several buspirone analogues have since been synthesized and tested for their 5-HT_{1A} receptor ligand affinity. However, to design new 5-HT_{1A} receptor ligands with high specificity and therapeutic potential in the treatment of anxiety or depression, more detailed knowledge about the three-dimensional structure of the 5-HT_{1A} receptor and the molecular mechanisms of ligands interacting with the 5-HT_{1A} receptor would be useful.

In this study, we have constructed a three-dimensional model of the 5-HT_{1A} receptor from its amino acid sequence, with the TMHs organized in an arrangement derived from the projection map of visual rhodopsin (Baldwin 1993; Schertler et al 1993; Unger & Schertler 1995). The model was used to study the molecular interactions of a series of buspirone analogues with the 5-HT_{1A} receptor by molecular-dynamics simulations and molecular-mechanical-energy minimization, and to calculate receptor-binding energies of the buspirone analogues.

Materials and Methods

Molecular-mechanical-energy minimization and molecular-dynamics simulation were performed with the Amber 4·0 programs. The Amber united atom force field (Weiner et al 1984) was used for the receptor model and the Amber all-atom force field (Weiner et al 1986) was used for the buspirone analogues. A distance-dependent dielectric function ($\varepsilon = r$; r is the inter-atomic distance), without explicit water molecules, was used in the calculations. The cut-off radius for non-bonded interactions was 12 Å in the energy minimization of the receptor model, buspirone analogues, and receptor–ligand complexes. The initial step-length in the minimization was

0·05, and the non-bonded pair list was updated after every 100 steps.

After an initial equilibrium period starting at 0·1 K, molecular-dynamics simulations with velocity scaling were performed at 310 K. The cut-off radius for non-bonded interactions was 8 Å during the simulations, and all bonds were constrained using the Shake option. The non-bonded pair list was updated after every 10 steps during the simulations. The step-length in the simulations was 0·001 ps, and coordinates were saved to a disk file at 1 ps intervals.

Modelling of ligands

The crystal structure of 4,4-dimethyl-1-{4-[4-2-quinolinyl)-1-piperazinyl]butyl}-2,6-piperidinedione (**1**) (Chilmonczyk et al 1995) was used as the starting structure for the preparation of initial all-atom models of the buspirone analogues (Fig. 1). The nitrogen atom attached to the butyl fragment was protonated for all analogues. The analogues were energy-minimized until convergence with a 0·02 kcal mol^{-1} Å energy gradient difference between successive steps.

Molecular-mechanics parameters for the buspirone analogues were initially set equal to standard all-atom Amber parameters, and adjusted to ensure reproduction of the main features of the crystal structure of **1**.

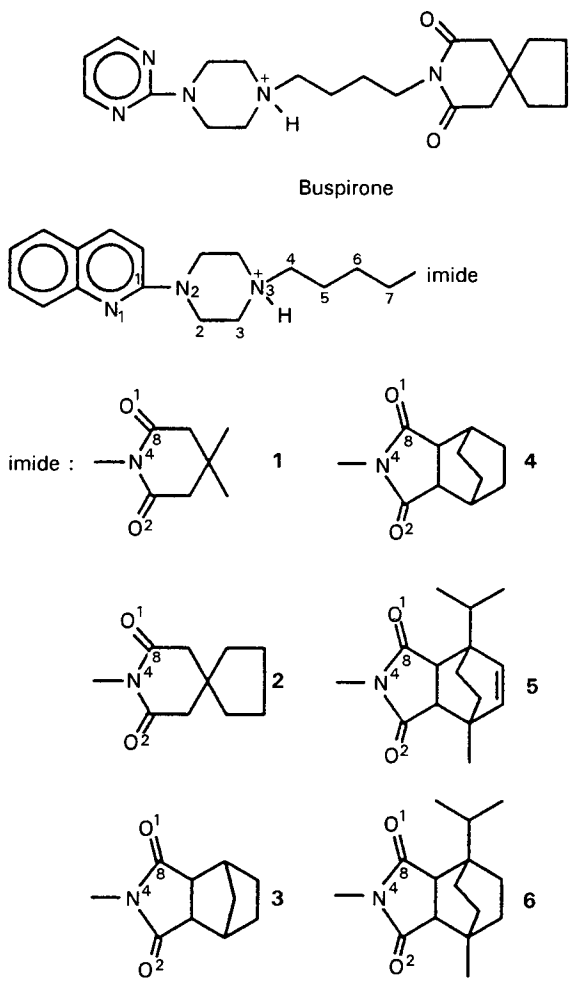

FIG. 1. Chemical structures of buspirone and analogues.

Atomic point charges for **1** were calculated by splitting the crystal structure, energy-minimized without electrostatic interactions, into two overlapping fragments. Fragment 1 consisted of the quinolinyl, piperazinyl and butyl groups. The butyl group was terminated in a hydrogen atom replacing the remaining part of **1**. Similarly, fragment 2 was created including the imide, butyl and piperazine groups, and piperazine was terminated with an extra hydrogen atom replacing the quinolinyl fragment. Each fragment was energy-minimized, and electrostatic-potential-based atomic point charges were calculated quantum mechanically with the Quest 1·0 program (Singh & Kollman 1984) using an STO-3G basis set. The atomic point charges were adjusted in the overlapping regions of fragments 1 and 2, and the crystal structure of **1** was energy-minimized with the atomic charges included. The r.m.s. difference between the crystal structure and the final energy-minimized structure was 0·29 Å.

The buspirone analogues were divided into four residues: quinolinyl, piperazinyl, butyl and different types of imide group (Fig. 1). From the calculated atomic point charges of **1**, standardized atomic point charges for the quinolinyl, piperazinyl and butyl residues were defined. The conformation resulting from energy minimization, and the corresponding standardized atomic point charges of the crystal structure of **1** were used for these residues in the other molecules in the series.

Atomic point charges for the imide groups were calculated by adding a butyl fragment to the nitrogen atom of the imide fragment. The butyl chain had the same conformation as in the energy-minimized crystal structure of **1**. Thus the only variation of molecular properties in the series was the substitution pattern, conformation and atomic point charges in the imide part of the molecule. (Molecular-mechanical parameters and atomic point charges for the buspirone analogues are available from the authors on request.)

Receptor modelling

The TMHs were constructed from the 5-HT$_{1A}$ receptor sequence in man (Chanda et al 1993) as α helices with ϕ and ψ angles of $-57°$ and $-47°$, respectively. Each TMH was refined by energy minimization and the helical bundle was organized according to the projection map of visual rhodopsin (Unger & Schertler 1995), using the arrangement of the TMHs in G protein-coupled receptors proposed by Baldwin (1993). The TMHs were organized such that amino acids in the 5-HT$_{1A}$ sequence at positions demonstrated to be important for ligand binding in other G protein-coupled receptors (Schwartz 1994; Baldwin 1994; van Rhee & Jacobson 1996) were facing the interior of the helical bundle. Few data are available about ligand binding to specific amino acids in TMH1 of G protein-coupled receptors. However, a threonine corresponding to Val57 in the 5-HT$_{1A}$ receptor has been shown to be important for agonist binding to bovine rhodopsin (Min et al 1993; Anukanth & Khorana 1994). Therefore, Val57, and Asn54 which are highly conserved among the G protein-coupled receptors (van Rhee & Jacobson 1996), were facing the interior of the helical bundle. In contrast with previous modelling of the 5-HT$_{1A}$ receptor (Sylte et al 1996), the water-accessible surface, electrostatic potentials and average hydrophobic moment of each TMH were not used in the packing of the helical bundle. Although both this and the previous model

were based on the projection map of visual rhodopsin, the significant difference in helix-packing strategy led to differences in the structure of the TMHs. In this model TMH3 was slightly less exposed to the lipid membrane, and TMH5 slightly more exposed, than in our previous model of the 5-HT_{1A} receptor (Sylte et al 1996). Seen from the extracellular side, the current model also differs from the previous model in that TMH6 was rotated 45° (clockwise) and TMH7 20° (clockwise), in order to take into account recent results from site-directed mutagenesis of G protein-coupled receptors (Baldwin 1994).

Loops and terminals were constructed, energy-refined and connected to the TMHs as described in our previous molecular-modelling study of the 5-HT_{1A} receptor interacting with various tetralin derivatives (Sylte et al 1996). After adding loops and terminals, the receptor model was energy-refined by 25 ps of molecular-dynamics simulation of the loops and terminals, while keeping the TMHs in a fixed position, then by energy minimization of the entire receptor model.

Simulation of receptor-1 interactions

Results from site-directed mutagenesis studies of the 5-HT_{1A} receptor (Guan et al 1992; Ho et al 1992; Chanda et al 1993) were used as a guide to dock the energy-minimized crystal structure of **1** into the receptor model in two different positions. In both positions, the protonated amino group (N3, Fig. 1) interacted with Asp116 in TMH3. In position 1, the imide group in **1** was orientated against TMH1, TMH2 and TMH7, with the carboxyl groups hydrogen-bonded with Ser86 in TMH2 and Ser393 in TMH7. The quinolinyl part of **1** was orientated towards TMH5 and TMH6. In position 2, the imide group was orientated towards the intracellular side of the receptor model, with the carbonyl groups hydrogen-bonded with Ser123 in TMH3 and Tyr400 in TMH7. The quinolinyl part interacted in an area between Ser86 in TMH2 and Ser393 in TMH7 on one side, and Phe112 in TMH3 and Tyr390 in TMH7 on the other side.

The two complexes of **1** and the receptor model were energy-minimized by 500 cycles of steepest-descent minimization then 2000 cycles of conjugate-gradient minimization. The complexes were further refined by 6 ps of molecular-dynamics simulation with the ligand and the amino acid side-chains free to move. The complexes obtained after 6 ps of simulation were used as start structures for 175 ps molecular-dynamics simulations without any constraints. The 25 coordinate sets saved between 150 and 175 ps were used to calculate average receptor-**1** complexes, which were energy-minimized. The molecular-interaction energy between amino acids in the receptor model and **1** were calculated for the energy-minimized average complexes.

Buspirone analogue-receptor binding energies

The three-dimensional structure of **1** in the energy-minimized average complexes was used as template for docking the buspirone analogues (Fig. 1) into the receptor model in two different positions relative to the receptor model. Each buspirone analogue was superimposed on to the structure of **1** in both complexes, and then **1** was removed from the complex. To obtain optimum matching between each ligand and **1**, rotation of ligand torsional angles was necessary. The ligand-receptor complexes and the ligand and receptor structures in each complex were energy-minimized until convergence with an energy gradient smaller than 0·02 kcal mol^{-1} Å. The binding energies (E_b) of the ligand-receptor complexes were calculated by use of the equation (Ferenczy & Morris 1989):

$$E_b = E_{int} + E_{LD} + E_{RD} \quad (1)$$

E_{int} is the total interaction energy between the ligand and the receptor in the energy-minimized complex. E_{LD} is the distortion energy of the ligand, calculated as the difference between the potential energy of the ligand molecule in the energy-minimized complex and that of the separately energy-minimized ligand molecule. E_{RD} is the distortion energy of the receptor, calculated as the difference between the potential energy of the receptor structure in the energy-minimized complex and that of the separately energy-minimized receptor structure.

Results

Three-dimensional structure of the receptor model

The use of the projection map of rhodopsin (Unger & Schertler 1995) and the proposed arrangement of the TMHs in G protein-coupled receptors (Baldwin 1993) as a guide in the helical packing introduced a hydrogen-bond between Asp82 in TMH2 and Asn396 in TMH7 (1·67 Å). The hydrogen-bond was retained during the molecular-dynamics simulations with **1** in the central core of the receptor model. In the average receptor-ligand complex with **1** in position 1, Asp82 was also hydrogen-bonded with Ser123 (1·68 Å) and Tyr400 in TMH7 (1·65 Å). In the average receptor-ligand complex with **1** in position 2, Asp82 was hydrogen-bonded to Asn396 only.

The main intention with the receptor-**1** simulations was not to study time-dependent structural changes but to overcome unfavourable non-bonded interactions and obtain energetically stable receptor-**1** complexes. Fig. 2 shows that energetically stable receptor-**1** complexes were obtained. Although several hydrogen-bonds involving Asp82 were formed during the simulations with **1** in position 1, the overall architecture of the TMHs was retained (Fig. 3). In both average complexes, kinks were seen in the region of Pro91 in TMH2, Pro170 and Pro171 in TMH4, Pro207 in TMH5, Pro360 in TMH6 and Pro397 in TMH7.

Receptor model-1 interactions

The molecular-interaction energies between **1** and specific amino acids in the receptor model are shown in Table 1. In the energy-minimized average complex with **1** in position 1, the carbonyl groups were still hydrogen-bonded with Ser86 in TMH2 and with Ser393 in TMH7. The remaining part of the imide group in **1** interacted with amino acids in TMH1, TMH2, TMH3 and TMH7. The quinolinyl group interacted in a pocket consisting of Ala365, Leu366, Cys371 and Glu372 in TMH6, and Ile385 in TMH7 (Fig. 4). The protonated nitrogen atom in the piperazine ring interacted strongly with Asp116 (Table 1) and the other nitrogen atom in the piperazine ring interacted close to the side chain of Phe362 in TMH6. The nitrogen atom in the heterocyclic ring system (Fig. 1) was located approximately 5 Å from the side-chain of Asp116.

With **1** in position 2, the initial hydrogen-bonds between the carbonyl groups and Ser123 in TMH3 and Tyr400 in TMH7 were not retained during the simulation. In the average com-

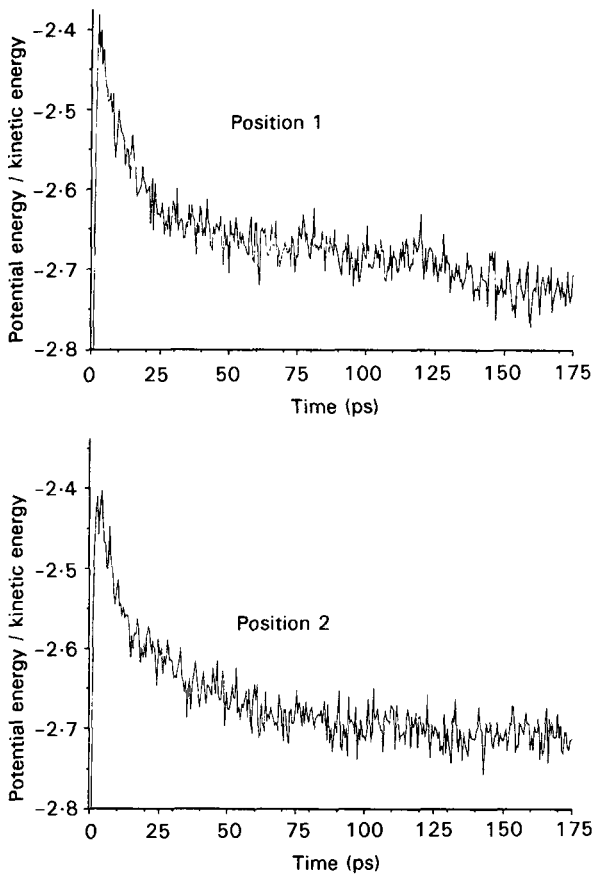

FIG. 2. Ratio between potential and kinetic energy of the receptor-ligand complexes during 175 ps of molecular-dynamics simulation.

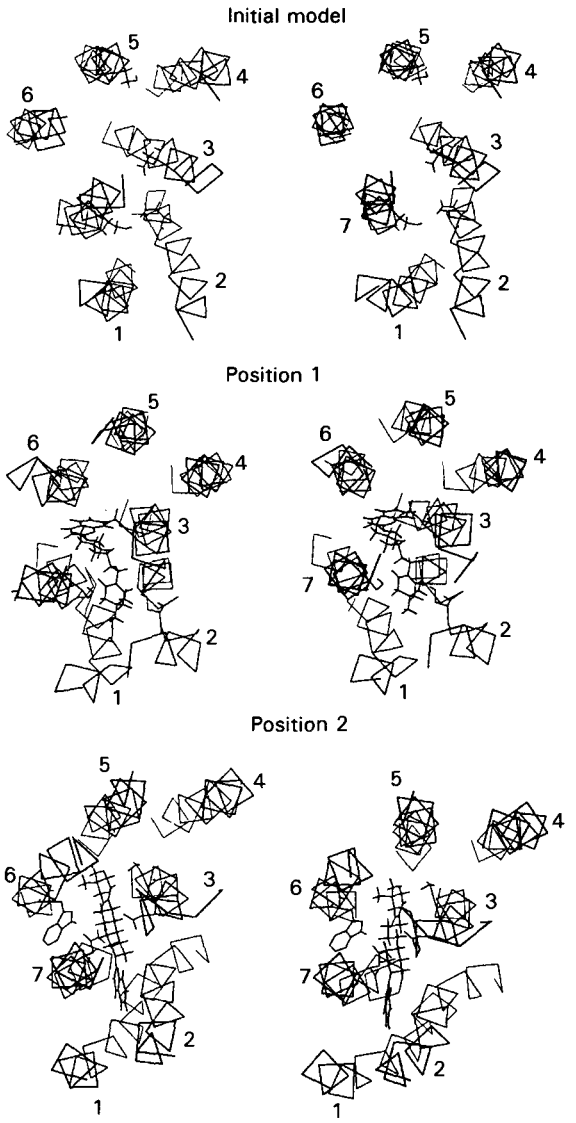

FIG. 3. Stereo view of the energy-minimized initial receptor model and of the energy-minimized average receptor-**1** complexes between 150 and 175 ps of simulation. C_α-atoms of the 7 TMHs are shown. Side-chains displayed: initial model; Asp82, Asp116, Ser199 and Ser393; position 1; Ser86, Asp116 and Ser393; position 2; Asp116, Cys120, Trp358 and Asn396.

plex, one of the carbonyl groups formed a hydrogen-bond with Cys120 in TMH3 and the other carbonyl group was involved in hydrogen-bonds with Trp358 in TMH6 and Asn396 in TMH7 (Fig. 4). The remaining part of the imide group in **1** interacted with amino acids in TMH3, TMH6 and TMH7. The protonated nitrogen atom in the piperazine ring interacted strongly with Asp116 and the quinolinyl part interacted in a pocket consisting of Val89 in TMH2, Phe112 in TMH3, Ile385, Asn386 and Tyr390 in TMH7.

Ligand-receptor binding energies

The calculations of ligand-receptor binding energies suggested that the buspirone analogues in position 1 bind to the receptor in the ranking order: **1** > **3** > **4** ≫ **2** > **6** > **5** as shown in Table 2. Except for (**6**), the theoretically calculated binding energies are in relatively good agreement with the ranking order of the experimentally determined inhibition constants of the buspirone analogues (Table 2). Table 3 indicates that the bulky imide group of **5** and **6** introduced greater structural changes in the region Leu88–Asn100 in TMH2 and the region Gly382–Leu395 in TMH7 than did the other buspirone analogues. Amino acids having van der Waals contact with the imide group of the buspirone analogues in position 1 are shown in Table 4.

The calculated ligand–receptor binding energies with the buspirone analogues in position 2 relative to the receptor model were not able to reproduce the ligand-binding ranking order from experimentally determined inhibition constants (Table 2), indicating that position 1 is the most realistic orientation of the buspirone analogues at the 5-HT$_{1A}$ receptor.

Structure of the buspirone analogues at the 5-HT$_{1A}$ receptor

Central intramolecular distances and torsional angles describing the receptor-bound conformation of the buspirone analogues in position 1 are shown in Table 5. In all buspirone analogue–receptor complexes, the piperazine ring (Fig. 1) had a chair conformation with the heterocyclic and butyl substituents in equatorial positions (Fig. 1). The buspirone analogues interacted with the receptor model in a rather folded conformation of the butyl chain (Table 5) compared with the crystal structure of **1**.

Table 1. Receptor-**1** interaction energies (kcal mol^{-1}) after energy-minimization of the average structure (average of coordinate sets between 150 and 175 ps of molecular-dynamics simulation). Amino acids with van der Waals contact with **1**, and other amino acids close to the ligand (contact after 20% increased van der Waals radii (*)) are included in the table.

Residue	Location	Position 1	Position 2
Leu43	TMH1	−1·4	–
Ile47	TMH1	−0·9(*)	–
Leu83	TMH2	−1·6	–
Ser86	TMH2	−4·9	−4·9
Val89	TMH2	–	−3·6
Leu90	TMH2	–	−2·1(*)
Ala93	TMH2	–	−0·3
Gln97	TMH2	−2·3	–
Cys109	EC1	−0·9	–
Phe112	TMH3	−11·3	−2·7
Ile113	TMH3	−3·8(*)	–
Leu115	TMH3	−2·8	–
Asp116	TMH3	−37·9	−48·4
Cys119	TMH3	−1·3(*)	1·9(*)
Cys120	TMH3	–	−4·9
Ser123	TMH3	–	−3·6
Leu127	TMH3	–	−1·2
Pro207	TMH5	–	−1·3
Ile355	TMH6	–	−2·4
Trp358	TMH6	–	−4·7
Phe361	TMH6	−1·6	−2·3
Phe362	TMH6	−3·7	−3·3
Ala365	TMH6	−2·3	–
Leu366	TMH6	−3·5	–
Cys371	TMH6	−1·0	–
Glu372	EC3	−4·8	–
Ile385	TMH7	−5·2	−4·3(*)
Asn386	TMH7	–	−5·7
Gly389	TMH7	−3·9	−1·5
Tyr390	TMH7	−3·9	−4·4
Asn392	TMH7	−3·5	−1·3
Ser393	TMH7	−2·7	–
Asn396	TMH7	–	−4·6
Tyr400	TMH7	–	−0·2(*)

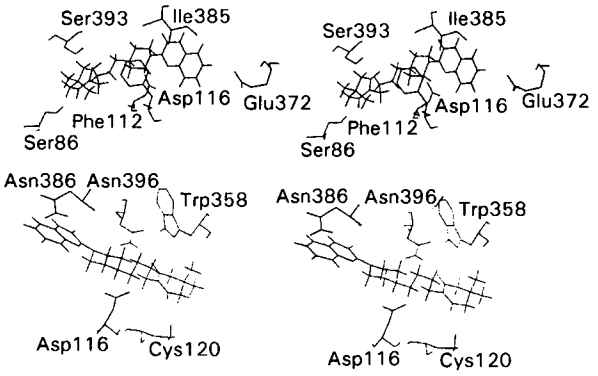

FIG. 4. Stereo view of the energy-minimized average **1**-receptor model complexes between 150 and 175 ps of simulation with **1** in position 1 (upper) and in position 2 (lower). The receptor is viewed from the extracellular side. The ligand and the most important amino acids for ligand binding are included in the figure.

Table 3. R.M.S. difference between the energy-minimized receptor-ligand complex and the receptor energy-minimized alone, calculated for segments in TMH2 and TMH7.

Ligand	Segment Leu88–Asn100 in TMH2	Ala383–Leu395 in TMH7
1	0·19	0·21
2	0·14	0·17
3	0·13	0·20
4	0·24	0·20
5	0·51	0·25
6	0·48	0·30

Discussion

Several models of monoamine G protein-coupled receptors have been constructed using the three-dimensional structure of bacteriorhodopsin (Henderson et al 1990) as a template for packing the TMHs. The projection maps showing the configuration of the TMHs of visual rhodopsin (Schertler et al 1993; Unger & Schertler 1995) indicate that the structure of rhodopsin is less elongated and slightly wider than the structure of bacteriorhodopsin, and that the TMHs are tilted differently. The projection maps of rhodopsin and the proposed arrangement of the TMHs in G protein-coupled receptors (Baldwin 1993) also suggest that TMH7 in rhodopsin is closer to TMH3 and TMH5 than in bacteriorhodopsin. It has also been shown that the use of bacteriorhodopsin as a template for packing the TMHs might ignore the fact that amino acids in TMH7 might

Table 2. Calculated interaction, distortion, and binding energies and experimental inhibition constants.

Position	Ligand	Total interaction energy between ligand and receptor in the energy-minimized complex	Distortion energy of the receptor upon binding (kcal mol^{-1})	Distortion energy of the ligand upon binding (kcal mol^{-1})	Calculated ligand-receptor binding energies (kcal mol^{-1})	Experimental inhibition constant (nM)
1	**1**	−126·2	11·1	2·0	−113·1	11 ± 2
	2	−128·7	13·7	4·1	−110·9	39 ± 7
	3	−129·3	13·6	3·9	−111·8	29 ± 4
	4	−129·5	14·4	4·3	−110·8	32 ± 7
	5	−136·5	26·8	7·3	−102·4	197 ± 12
	6	−138·9	24·5	6·3	−108·0	1262 ± 129
2	**1**	−129·0	22·4	2·0	−104·6	11 ± 2
	2	−131·0	30·7	1·9	−98·4	39 ± 7
	3	−127·1	25·7	2·0	−99·4	29 ± 4
	4	−129·2	26·7	3·4	−99·1	32 ± 7
	5	−141·4	22·3	0·0	−119·1	197 ± 12
	6	−140·5	29·6	4·4	−106·5	1262 ± 129

Experimental inhibition constants are given as mean ± s.e.m. (Chilmonczyk et al, unpublished work).

Table 4. Molecular-interaction energies (kcal mol^{-1}) between the imide group of the buspirone analogues (Fig. 1) in position 1 and amino acids in the receptor model.

Amino acid	TMH	Ligand					
		1	**2**	**3**	**4**	**5**	**6**
Leu43	1	−1·3	−1·4	−1·7	−1·2	−1·6	−1·2
Leu83	2	−0·9	−0·9	−0·7		−1·2	−1·1
Ser86	2	−4·9	−5·1	−5·5	−5·3	−5·5	−6·0
Ala93	2		−1·5	−0·9		−0·2	−0·8
Gln97	2		−2·0	−2·0	−2·0	−3·8	−3·0
Phe112	3	−2·2	−2·1	−2·3	−2·2		
Leu115	3	−2·0	−2·4	−2·4	−2·6	−2·7	−3·3
Asn386	7					−2·3	
Gly389	7					−2·0	−2·6
Tyr390	7	−3·1	−3·4	−3·7	−3·4	−4·8	−4·6
Asn392	7		−0·5				
Ser393	7	−2·9	−2·9	−2·8	−3·0	−2·9	−2·8

Only amino acids having van der Waals contact with the imide group after energy minimization of the receptor–ligand complexes are included in the table.

be involved in ligand binding (Donnelly et al 1994). The validity of the final conclusions from such models regarding ligand binding and the quality of molecular-dynamics simulations of receptor–ligand interactions rely heavily on the initial model of the receptor. The structural differences between bacteriorhodopsin and rhodopsin, and the fact that in contrast with bacteriorhodopsin, rhodopsin is a G protein-coupled receptor, suggest that a model of an aminergic G protein-coupled receptor should be based on the electron-density projection map of rhodopsin rather than on the structure of bacteriorhodopsin.

Although our present and previous (Sylte et al 1996) models of the 5-HT$_{1A}$ receptor are both based on the projection map of visual rhodopsin, the significant difference in helix-packing strategy led to differences in the structure of the TMHs of these models. However, the initial structure of the 7 TMHs in the current model (Fig. 3) was in better agreement with the projection map of rhodopsin (Unger & Schertler 1995) and the proposed arrangement of the TMHs in G protein-coupled receptors (Baldwin 1993) than the 7 TMHs in our previous rhodopsin-based model of the 5-HT$_{1A}$ receptor (Sylte et al 1996).

The strategy for packing of the TMHs introduced a hydrogen-bond between Asp82 in TMH2 and Asn396 in TMH7. These amino acids are highly conserved among the G protein-coupled receptors, and site-directed mutagenesis studies have suggested that these amino acids are involved in a common hydrogen-bonding network underlying receptor activation by agonists both in the gonadotropin-releasing-hormone receptor (Zhou et al 1994) and the 5-HT$_{2A}$ receptor (Sealfon et al 1995).

In the energy-minimized average complex with **1** in position 1, Asp82 and Asn396 were involved in a hydrogen-bonding network also consisting of Ser123 in TMH3, and Tyr400 in TMH7. The molecular-dynamics simulation of **1**-receptor interactions introduced kinks in some of the TMHs (Fig. 3). The largest kinks were introduced in the region of highly conserved proline residues located at the same depth in TMH2, TMH4, TMH5, TMH6 and TMH7, where they appear to surround the ligand-binding pocket. It seems likely, therefore, that ligand-induced conformational changes in the TMHs and the formation or breaking of a hydrogen-bonding network consisting of Asp82, Asn396 and probably also Ser123 and Tyr400, are important for the activation of the receptor. This hypothesis is supported by site-directed mutagenesis studies of the highly conserved proline in TMH7 of the muscarinic m3 receptor which resulted in a receptor still able to bind the agonist but with severely impaired ability to activate its second messenger pathway (Wess et al 1993).

The method for calculating the microscopic ligand–receptor binding energies in this study has certain limitations. In aqueous solution, one driving force for binding is the increase of entropy owing to disappearance of ordered water–ligand and water–receptor contacts; this is not taken into account in the present method. Another possible limitation is the structural accuracy of the receptor model. However, the calculated microscopic binding energies do take into account structural changes both in the receptor and the ligand during binding, and might therefore be expected to be better correlated to experimental binding data than the molecular-interaction energy (E_{int}) between the receptor and the ligand. The most widely accepted model for agonist binding to G protein-coupled monoamine receptors suggests that the protonated amino group of the ligand interacts with the highly conserved aspartic acid residue in TMH3, whereas other parts of the ligand interact with amino acids near to the synaptic end of TMH5, TMH6 and TMH7 (Schwartz 1994). Such a binding model has also been suggested for the 5-HT$_{1A}$ receptor (Kuipers et al 1995) and the buspirone analogues interacting with the receptor in position 1 are in accordance with that model (Fig. 4). An alternative model for ligand binding to the monoamine G protein-coupled receptors has also been suggested (Hutchins 1994), wherein the ligand interacts deeply in a binding pocket between TMH2, TMH3 and TMH7. Position 2 of the buspirone analogues interacting with the receptor are in accordance with that model (Fig. 4).

The quantitative relationship between the binding affinity and the calculated binding energies for the buspirone analo-

Table 5. Intramolecular distances (Å) and torsional angles (°) of the buspirone analogues after complexation with the 5-HT$_{1A}$ model.

	1	**2**	**3**	**4**	**5**	**6**
Centre of heterocyclic ring ··· $N3^+$ (d)	5·65	5·65	5·65	5·65	5·66	5·65
Deviation of $N3^+$ from the heterocyclic ring plane (h)	0·39	0·26	0·20	0·12	0·19	0·12
Torsional angle: N1-C1-N2-C2 (T1)	5·4	4·1	5·8	3·8	4·4	5·5
Torsional angle: C3-$N3^+$-C4-C5 (T2)	166·1	164·3	161·3	159·1	167·6	162·2
Torsional angle: $N3^+$-C4-C5-C6 (T3)	125·3	127·6	132·5	130·8	131·1	129·4
Torsional angle: C4-C5-C6-C7 (T4)	261·9	266·6	268·7	265·6	259·5	262·4
Torsional angle: C5-C6-C7-N4 (T5)	145·2	143·7	135·0	135·2	131·2	135·6
Torsional angle: C6-C7-N4-C8 (T6)	280·0	273·0	261·7	275·5	288·7	284·1

gues (Table 2) clearly supports orientation of the buspirone analogues similar to the most widely accepted model of ligand binding, with the buspirone analogues interacting at the extracelluar ends of the TMHs (Fig. 4). Asn386 has been found not to be important for binding of buspirone to the 5-HT_{1A} receptor (Ho et al 1992). In position 2 Asn386 interacts with **1** (Table 1), which further supports position 1 rather than position 2 as the most realistic position of the buspirone analogues in the receptor. With the buspirone analogues in position 1, the quinolinyl group interacted in a pocket consisting of Ala365, Leu366, Cys371 and Glu372 in TMH6, and Ile385 in TMH7 (Fig. 4). The piperazine ring interacted with Asp116 in TMH3, Phe362 in TMH6, Leu388, Gly389 and Asn392 in TMH7, while the imide group interacted mainly with Leu43 in TMH1, Leu83, Ser86 in TMH2, Phe112, Leu115 in TMH3, and Tyr390 and Ser393 in TMH7 (Table 4).

A proposed general model for 5-HT_{1A} receptor-binding places a basic nitrogen atom at a distance of 5·2–5·8 Å from the centroid of an aromatic ring, in the range of 0·9 Å below the plane of the aromatic ring to 1·5 Å above the plane (Bolis et al 1995). These distances correspond to parameters d and h in Table 5. Furthermore, it has been suggested that the out-of-plane-deviation between the aromatic ring and the basic nitrogen atom is 1·6 Å for antagonists, and 0·2 Å for agonists (Hibert et al 1988, 1989). Table 5 indicates that the receptor-bound conformation of the buspirone analogues satisfies the postulated pharmacophore requirements for 5-HT_{1A}-receptor agonists. Pharmacological studies have shown that buspirone is a partial agonist at the 5-HT_{1A} receptor (Traber & Glaser 1987). The structural similarities of the present analogues with buspirone, their affinity for the 5-HT_{1A} receptor (Table 2) and their receptor-bound conformation which satisfies the proposed agonist pharmacophore (Table 5), suggest that **1**, **2**, **3** and **4** might all have receptor-binding profiles similar to that of buspirone.

The variation in the measured binding constants is well accounted for by the calculated receptor-binding energies of the buspirone analogues in position 1 (Table 2). In position 1, the changes in potential energy of the receptor upon formation of the ligand–receptor complex are mainly responsible for the differences in binding energy between the buspirone analogues (Table 2). This might suggest that steric hindrance and repulsive forces between the receptor and the imide group, which is the structurally divergent part of these ligands (Fig. 1), play the most important role for discriminating between the ligands. The bulky imide group of **5** and **6** (Fig. 1) introduced greater conformational changes in TMH2 and TMH7 than did the other buspirone analogues (Table 3). The more favourable interaction energies of **5** and **6** with Gln97 in TMH2, Leu115 in TMH3, Asn386, Gly389 and Tyr390 in TMH7 than the other buspirone analogues (Table 4), were not able to overcome the increase in potential energy as a result of conformational changes in this part of the receptor (Table 2). Thus, from a dynamic point of view, greater reorganization of the structural architecture of Leu83, Ser86, Ala93 and Gln97 in TMH2, Asn386, Gly389, and Tyr390 in TMH7 appear to be necessary for accommodating the binding of **5** and **6** to the receptor than for the binding of the other buspirone analogues.

The current model of ligand-5-HT_{1A}-receptor interactions might provide a useful approach for further experimental studies of the 5-HT_{1A} receptor by protein-engineering experiments. Furthermore, the relatively detailed picture of the buspirone analogue–receptor interactions emerging from the current study might be useful for designing new ligands with potential anxiolytic or anti-depressive effects.

Acknowledgements

This work was supported by the Norwegian Research Council, the Norwegian Supercomputing Committee and the L. F. Saugstad Research Foundation.

References

Anukanth, A., Khorana, H. G. (1994) Structure and function of rhodopsin. Requirements of a specific structure for the intradiscal domain. J. Biol. Chem. 269: 19738–19744

Baldwin, J. M. (1993) The probable arrangement of the helices in G protein-coupled receptors. EMBO J. 12: 1693–1703

Baldwin, J. M. (1994) Structure and function of receptors coupled to G proteins. Curr. Opin. Cell Biol. 6: 180–190

Bolis, G., Pillan, A., Mantegani, S., Brambilla, E., Dolmella, A. (1995) Ergoline derivatives as a probe for featuring the 5-HT_{1A} receptor pharmacophore. J. Mol. Model. 1: 188–195

Chanda, P. K., Minchin, M. C. W., Davies, A. R., Greenberg, L., Reilly, Y., McGregor, W. H., Bhat, R., Lubeck, M. D., Mitzutani, S., Hung, P. P. (1993) Identification of residues important for ligand binding to the human 5-hydroxytryptamine$_{1a}$ serotonin receptors. Mol. Pharmacol. 43: 516–520

Chilmonczyk, Z., Les, A., Wozniakowska, A., Cybulski, J., Koziol, A. E., Gdaniec, M. (1995) Buspirone analogues as ligands of the 5-HT_{1A} receptor. 1. The molecular structure of buspirone and its two analogues. J. Med. Chem. 38: 1701–1710

Donnelly, D., Findlay, J. B. C., Blundell, T. L. (1994) The evolution and structure of aminergic G protein-coupled receptors. Receptors and Channels 2: 61–78

Ferenczy, G. F., Morris, G. M. (1989) The active site of cytochrome P-450 nifedipine oxidase: a model building study. J. Mol. Graphics 7: 206–211

Goa, K. L., Ward, A. (1986) Buspirone: a preliminary review of its pharmacological properties and therapeutic efficacy as an anxiolytic. Drugs 32: 114–129

Guan, X.-M., Peroutka, S. J., Kobilka, B. K. (1992) Identification of a single amino acid residue responsible for the binding of a class of β-adrenergic receptor antagonists to the 5-hydroxytryptamine$_{1A}$ receptors. Mol. Pharmacol. 41: 695–698

Henderson, R., Baldwin, J. M., Ceska, T. A., Zemlin, F., Beckman, E., Downing, K. H. (1990) Model for the structure of bacteriorhodopsin based on high-resolution electron cryo-microscopy. J. Mol. Biol. 213: 899–929

Hibert, M. F., Gittos, M. W., Middlemiss, D. N., Mir, A. K., Fozard, J. R. (1988) Graphics computer-aided receptor mapping as a predictive tool for drug design: development of potent, selective, and stereospecific ligands for the 5-HT_{1A} receptor. J. Med. Chem. 31: 1087–1093

Hibert, M. F., McDermott, I., Middlemiss, D. N., Mir, A. K., Fozard, J. R. (1989) Radioligand binding study of series of 5-HT_{1A} receptor agonists and definition of a steric model of this site. Eur. J. Med. Chem. 24: 31–37

Ho, B. Y., Karschin, A., Branchek, T., Davidson, N., Lester, H. A. (1992) The role of conserved aspartate and serine residues in ligand binding and its function of the 5-HT_{1A} receptor: a site-directed mutation study. FEBS Lett. 312: 259–262

Hoyer, D., Clarke, D. E., Fozard, J. R., Hartig, P. R., Martin, G. R., Mylecharane, E. J., Saxena, P. R., Humphrey, P. A. (1994) VII. International Union of Pharmacology classification of receptors for 5-hydroxytryptamine (serotonin). Pharmacol. Rev. 46: 157–203

Hutchins, C. (1994) Three-dimensional model of the D_1 and D_2 dopamine receptors. Endocrine J. 2: 7–23

Kuipers, W., Van Wijngaarden, I., Kruse, C. G., ter Horst van Amstel, M., Tulp, M. T., Ijzerman, A. P. (1995) N^4-Unsubstituted N^1-arylpiperazines as high-affinity 5-HT_{1A} receptor ligands. J. Med. Chem. 38: 1942–1954

Min, K. C., Zvyaga, T. A., Cypess, A. M., Sakmar, T. P. (1993)

Characterization of mutant rhodopsin responsible for autosomal dominant retinitis pigmentosa. Mutations on the cytoplasmic surface affect transducin activation. J. Biol. Chem. 268: 9400–9404

Peroutka, S. J. (1995) Serotonin receptors. Their evolution and clinical relevance. CNS Drugs 4 (Suppl. 1): 18–28

Schertler, G. F. X., Villa, C., Henderson, R. (1993) Projection structure of rhodopsin. Nature 362: 770–772

Schwartz, T. W. (1994) Locating ligand-binding sites in 7TM receptors by protein engineering. Curr. Opin. Biotech. 5: 434–444

Sealfon, S. C., Chi, L., Ebersole, B. J., Rodie, V., Zhang, D., Ballesteros, J. A., Weinstein, H. (1995) Related contribution of specific helix 2 and 7 residues to conformational activation of the serotonin 5-HT$_{2A}$ receptors. J. Biol. Chem. 270: 16683–16688

Singh, U. C., Kollman, P. A. (1984) An approach to computing electrostatic charges for molecules. J. Comput. Chem. 5: 129–145

Sylte, I., Edvardsen, Ø., Dahl, S. G. (1996) Molecular modelling of UH-301 and 5-HT$_{1A}$ receptor interactions. Protein Eng. 9: 149–160

Traber, J., Glaser, T. (1987) 5-HT$_{1A}$ receptor-related anxiolytics. Trends Pharmacol. Sci. 8: 432–437

Unger, V. M., Schertler, G. F. X. (1995) Low resolution structure of bovine rhodopsin determined by electron cryo-microscopy. Biophys. J. 68: 1776–1786

van Rhee, A. M., Jacobson, K. A. (1996) Molecular architecture of G protein-coupled receptors. Drug. Dev. Res. 37: 1–38

Weiner, S. J., Kollman, P. A., Case, D. A., Singh, U. C., Ghio, C., Alagona, G., Profeta Jr, S., Weiner, P. (1984) A new force field for molecular mechanical simulation of nucleic acids and proteins. J. Am. Chem. Soc. 106: 765–784

Weiner, S. J., Kollmann, P. A., Nguyen, D. T., Case, D. A. (1986) An all-atom force field for simulation of proteins and nucleic acids. J. Comput. Chem. 7: 230–252

Wess, J., Nanavati, S., Vogel, Z., Maggio, R. (1993) Functional role of proline and tryptophan residues highly conserved among G protein-coupled receptors studied by mutational analysis of the m3 muscarinic receptor. EMBO J. 12: 331–338

Wieland, S., Lucki, I. (1990) Antidepressant-like activity of 5-HT$_{1A}$ agonists measured with the forced swim test. Psychopharmacology 101: 497–504

Zhou, W., Flanagan, C., Ballesteros, J. A., Konvicka, K., Davidson, J. S., Weinstein, H., Millar, R. P., Sealfon, S. C. (1994) Replacement of lysine-181 by aspartic acid in the third trans-membrane region of endothelin type B receptor reduces its affinity to endothelin peptides and sarafotoxin 6c without affecting G protein coupling. Mol. Pharmacol. 45: 165–170